Vorticity and vortex-core states in type-II superconductors

C. Berthod

DPMC, Université de Genève, 24 quai Ernest-Ansermet, 1211 Genève 4, Switzerland
(Received 22 January 2004; revised manuscript received 4 June 2004; published 20 April 2005)

The origin of the vortex-core states in s-wave and $d_{x^2-y^2}$-wave superconductors is investigated by means of some selected numerical experiments. By relaxing the self-consistency condition in the Bogoliubov–de Gennes equations and tuning the order parameter in the core region, it is shown that the suppression of the superfluid density in the core is not a necessary condition for the core states to form. This excludes "potential well" types of interpretations for the core states. The topological defect in the phase of the order parameter, however, plays a crucial role. This fact is explained by considering the effect of the vortex supercurrent on the Bogoliubov quasiparticles and illustrated by comparing conventional vortices to multiply quantized vortices and vortex-antivortex pairs. The core states are also found to be extremely robust against random disorder of the phase.

I. INTRODUCTION

The vortices govern the electromagnetic response of type-II superconductors and have been extensively studied, both experimentally and theoretically.[1,2] A vortex is formed from a core of radius $r_c \sim \xi$ where the superfluid density is gradually suppressed, ξ the superconducting coherence length, and it is surrounded by a supercurrent that screens the magnetic field on a length of order λ, the penetration depth. The vortices are strong inhomogeneities of the superconducting condensate, and they scatter the quasiparticles in several different ways.[3] In particular, the vortices can capture Bogoliubov excitations into low-energy localized states.

The vortex-core states play an important role in the thermodynamic and transport properties in the mixed state. For example, when vortices move in an applied electric field, the core states interact with the lattice and are thus responsible for the dissipation of energy. These states are also affected by localized perturbations, and they contribute to the pinning of vortices by defects or impurities. Recently, mesoscopic superconducting disks have attracted much attention.[4] In these systems a "giant-vortex state" can be stabilized, in which a single vortex at the center of the sample carries the whole magnetic flux. In such a case the core states are the main low-energy excitations and are expected to play a dominant role. Furthermore, the strong dependence of the vortex-core energy spectrum on the applied magnetic field opens interesting perspectives for applications.[5]

In s-wave superconductors the vortex-core bound states were predicted long ago, based on approximate solutions of the microscopic Bogoliubov–de Gennes (BdG) equations,[6,7] and subsequently observed in NbSe$_2$ using scanning tunneling spectroscopy.[8] The early analytical results were confirmed by a complete numerical solution of the BdG equations.[9] Extended quasiparticle excitations in the mixed state were often studied within the quasiclassical approach.[2,10] Although this approximation is considered inaccurate near the vortex core, it was used by Volovik to argue that the number of branches of core states crossing the Fermi energy as a function of angular momentum (considered as a continuous variable) is equal to the winding number of the vortex.[11] This prediction was confirmed recently

by a detailed numerical solution of the BdG equations for multiply quantized vortices.[12] The vortex-core states are usually thought of as Andreev bound states, i.e., standing waves resulting from the multiple Andreev reflection at the normal-superconductor boundary in the core.[2,10,13,14] This interpretation suggests that the suppression of the superfluid density in the core is the main reason for the formation of the core states. The vanishing of the superfluid density in the core, however, plays no role in Volovik's argument. Instead, the structure of the vortex-core energy spectrum in the approach of Ref. 11 is entirely determined by the winding number of the vortex, which measures the strength of the supercurrent circulating around it. This result seems difficult to reconcile with the Andreev-bound state picture. In particular, the peculiar dependence of the spectrum of core states on vorticity[12] can hardly be attributed to the order-parameter suppression alone. Hence it is of interest to identify the roles played by the supercurrent, on the one hand, and by the order-parameter suppression, on the other hand, in the formation of the vortex-core states.

Based on numerical and analytical solutions of the microscopic BdG equations, we show that the structure of the bound-state spectrum in s-wave and d-wave vortices is determined by a topological constraint that the circulating superfluid imposes to Bogoliubov quasiparticles, consistently with Volovik's result. The suppression of the order parameter in the core plays a minor quantitative role, slightly changing the energy of the states with small angular momenta. This implies, in particular, that a complete self-consistent treatment of the order-parameter profile is, in general, not necessary, unless one is interested in detailed quantitative predictions. These results suggest that the mechanism leading to quasiparticle localization in vortices is quite different from other localization mechanisms in condensed matter.

II. TOPOLOGY OF VORTICES AND BdG EQUATIONS

A vortex is a topologically stable defect of the superconducting order parameter $\Psi(\boldsymbol{r}) \equiv \Delta(\boldsymbol{r}) e^{i\chi(\boldsymbol{r})}$.[15] It is characterized by a winding number ν, a topological invariant defined as

$$\nu = \frac{1}{2\pi} \oint \boldsymbol{\nabla} \chi \cdot d\boldsymbol{l}. \tag{1}$$

The integral runs along a closed path around the vortex axis. $|\nu|$ counts the number of 2π rotations of the phase $\chi(\boldsymbol{r})$ along the path. Clearly ν is invariant under all continuous distortions of the phase. Except near surfaces or interfaces, ν corresponds to the magnetic flux Φ carried by the vortex according to $\Phi = \nu \Phi_0$ with $\Phi_0 = h/2e$ the superconducting flux quantum. Another characteristics of the vortex is the shape of the order-parameter modulus $\Delta(\boldsymbol{r})$ in the vicinity of the vortex axis, where it is constrained to vanish.

For an isolated axisymmetric vortex in a s-wave superconductor one has $\Delta(r,\theta,z) \equiv \Delta(r)$ and $\chi(r,\theta,z) = \nu\theta$, where ν is the winding number consistently with Eq. (1). The modulus $\Delta(r)$ vanishes as $r \to 0$, and approaches the constant value Δ_∞ at $r > r_c$, where $r_c \sim \xi \ll \lambda$ in type-II superconductors. The excitation spectrum of the vortex is determined by the Bogoliubov–de Gennes (BdG) equations,

$$\begin{pmatrix} \hat{h} & \Psi \\ \Psi^\star & -\hat{h}^\star \end{pmatrix} \begin{pmatrix} u \\ v \end{pmatrix} = E \begin{pmatrix} u \\ v \end{pmatrix}, \tag{2}$$

where $\hat{h} = 1/2m(\boldsymbol{p} - e\boldsymbol{A})^2 - E_F$ and u (v) is the electron (hole) wave function of the excitation. In order to solve Eq. (2) one usually eliminates the phase χ of the order parameter from the off-diagonal terms by performing the gauge transformation $\boldsymbol{A} \to \boldsymbol{A} - (\hbar/2e)\boldsymbol{\nabla}\chi$. The order parameter changes according to $\Psi \to \Psi e^{-i\chi}$ and thus becomes real.[6] This transformation is achieved by writing the wave functions as

$$\begin{bmatrix} u(\boldsymbol{r}) \\ v(\boldsymbol{r}) \end{bmatrix} = \begin{bmatrix} e^{ik_z z} e^{i(\mu+\nu/2)\theta} \psi_+(r/\xi) \\ e^{ik_z z} e^{i(\mu-\nu/2)\theta} \psi_-(r/\xi) \end{bmatrix}. \tag{3}$$

The phase $\pm(\nu/2)\theta$ in Eq. (3) is an Aharonov-Bohm phase, reflecting the fact that the gauge function $-\frac{1}{2}\chi$ carries a singular magnetic field at the origin.[16] Furthermore, the quantum number μ must be such that the total phase accumulated by the electron and hole upon a 2π rotation around the origin is consistent with the enclosed flux, i.e.,

$$\mu = n + \frac{\nu}{2}, \quad n \text{ integer}. \tag{4}$$

Inserting Eq. (3) into Eq. (2) solves for the θ and z dependencies and leads to the radial equations for the real functions $\psi_\pm$:

$$\pm L_\pm \psi_\pm(\rho) + \delta(\rho)\psi_\mp(\rho) = \varepsilon\psi_\pm(\rho) \tag{5a}$$

$$L_\pm = \frac{1}{g^2} \left\{ -\frac{d^2}{d\rho^2} - \frac{1}{\rho}\frac{d}{d\rho} + \frac{[\mu \pm (\nu/2)]^2}{\rho^2} \right\} - 1. \tag{5b}$$

Here $g = k_F\xi$ and we have introduced the dimensionless variables $\rho = r/\xi$, $\varepsilon = E/E_F$, and $\delta(\rho) = \Delta(\rho\xi)/E_F$. For simplicity we restricted, in Eq. (5b), to the two-dimensional case by putting $k_z = 0$. The vector potential $\boldsymbol{A}$ was also omitted since it is small in the core region compared to the gauge field $(\hbar/2e)\boldsymbol{\nabla}\chi$ when $\lambda \gg \xi$.[6] Indeed $A \sim (\nu\Phi_0/4\pi\lambda^2)r$, and the ratio of A to the gauge field is thus of order $(r/\lambda)^2$.

Although the gauge transformation removes the phase of the order parameter, it does not eliminate the supercurrent from the problem. In the radial equation, the supercurrent shows up as a central potential containing a repulsive term $(\nu/2\rho)^2$, as well as a term $\pm\mu\nu/\rho^2$, which is either attractive or repulsive: if $\nu < 0$ (supercurrent flowing counterclockwise, corresponding to a positive magnetic field along the z axis) this term is attractive (repulsive) for the electrons (holes) that move like the superfluid ($\mu > 0$). Therefore, the supercurrent acts on the electron and hole parts of the BdG excitations in different ways, and tends to decrease the angular momentum of the former and to increase the angular momentum of the latter (for $\nu < 0$ and $\mu > 0$). This effect of the supercurrent on the BdG excitations is central to understand the formation of the core states (see Sec. III B). Furthermore, the strength of the supercurrent fixes the parity of the vortex-states angular momentum in Eq. (4), which is half an odd integer for odd ν and integer for even ν. When ν is odd, the flux carried by the vortex is not a multiple of the flux carried by the quasiparticle, hence a topological frustration which translates into a branch cut discontinuity— removed by the gauge transformation in Eq. (3)—in the angular wave function.

Equation (2) possesses the well-known particle-hole symmetry $(u,v,E) \leftrightarrow (v^*,-u^*,-E)$. Looking at the wave functions in Eq. (3), one sees that in the radial equation this symmetry becomes $(\mu,\psi_+,\psi_-,\varepsilon) \leftrightarrow (-\mu,\psi_-,-\psi_+,-\varepsilon)$: the vortex-core energy spectrum is invariant under the simultaneous inversion of angular momentum and energy. Furthermore, it is clear from Eq. (5) that the spectrum is also invariant under the simultaneous inversion of μ and ν.

III. ISOLATED S-WAVE VORTEX

Self-consistent solutions of the BdG equations for the order-parameter profile and the energy spectrum of an isolated s-wave vortex were already reported, both in the singly quantized[9] and multiply quantized[12] cases. The purpose of this section is to repeat these calculations without achieving the self-consistency in $\Delta(r)$, in order to clarify the role played by the detailed form of $\Delta(r)$ and by the winding number ν in the formation of the core states. Analytical solutions for the singly quantized vortex also exist.[6,7] We will discuss an analytical solution that is valid for all (integer) values of ν and that emphasizes the key role of the winding number.

A. Numerical results

The BdG equations (5) were solved numerically using the Bessel-function expansion described in Ref. 9. Besides its winding number and order-parameter profile, an isolated vortex in a continuum free-electron model is characterized by the bulk parameters $g = k_F\xi$ and $\delta = \Delta_\infty/E_F$. Physical values of g range from ~ 1 in high-T_c materials to 10–10^4 in conventional superconductors. Simulations were performed for g between 1 and 100 (the computational effort increases rapidly with increasing g). The parameters g and δ are in principle related by the BCS relation $\xi \approx \hbar v_F/\pi\Delta_\infty$, i.e., $g\delta \approx 2/\pi$. For each g, values of δ between 0.1 and 10 times the

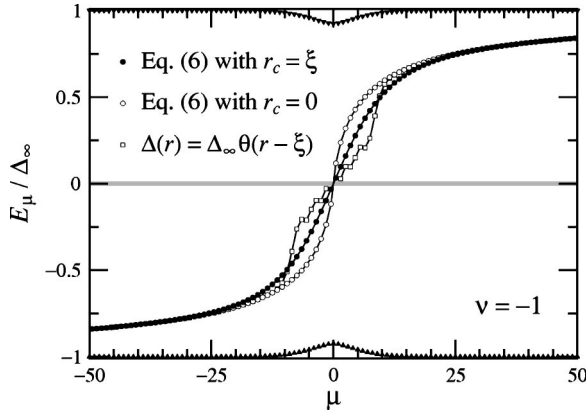FIG. 1. Subgap energy spectrum of a singly quantized s-wave vortex as a function of angular momentum μ for various order-parameter profiles in the core: nearly self-consistent profile (black circles), "no-core" profile (white circles), and steplike profile (squares). The triangles show the energy spectrum of a normal region analogous to a vortex core embedded in a uniform superconductor (no supercurrent).
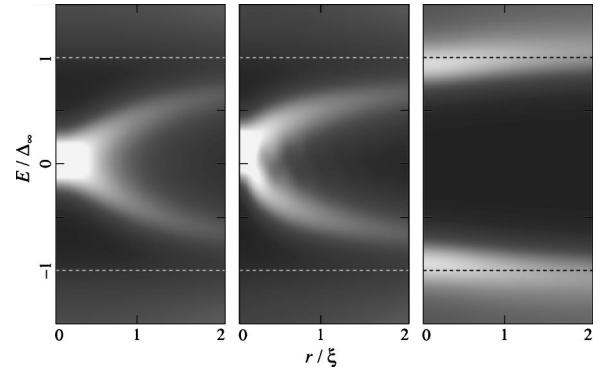

FIG. 2. Local density of states for the systems shown in Fig. 1: conventional singly quantized vortex (left), vortex without normal core (center), and normal core without supercurrent (right). A thermal broadening was used with $k_B T = \Delta_\infty / 10$.

BCS value were considered. The reported conclusions apply to the whole domain of parameters investigated. Below we present results for $g=10$ and $\delta=2/(\pi g)$.[17] For the order-parameter profile the following form was used:[18]

$$\Delta(r) = \Delta_\infty \tanh\left(\frac{r}{\sqrt{|\nu|}r_c}\right)^{|\nu|}. \qquad (6)$$

This functional form with $r_c = \xi$ is in good qualitative agreement with the self-consistent results of Ref. 12. By tuning the value of r_c one can study the effect of the gap profile on the vortex-core spectrum. In particular, the limit $r_c \rightarrow 0$ corresponds to a vortex with no normal core. (In the remainder of this paper, we use the expression *normal core* as a synonym for *suppression of* $\Delta(r)$ *in the vortex core*.) According to the Andreev-reflection picture, one may expect that reducing the core radius will increase the energy separation between the vortex-core energy levels and eventually push the core states outside the energy gap into the continuum as $r_c \rightarrow 0$.

The spectra of subgap states for a singly quantized vortex ($\nu = -1$) and for gap profiles corresponding to $r_c = \xi$ and $r_c = 0$ are shown in Fig. 1. The eigenvalues are displayed as a function of the angular quantum number μ. At energies outside the superconducting gap, the BdG states form a continuum not shown in the figure. The spectrum obtained for a steplike profile $\Delta(r) = \Delta_\infty \theta(r - \xi)$, which is often used in analytical calculations, is also displayed for comparison. The spectra are similar in all three cases, except for small differences at low values of $|\mu|$. These differences have a rather simple explanation: the corresponding eigenstates are concentrated close to the vortex axis (the maximum of the wave function lies roughly at position $|\mu|/g$ in units of ξ); thus the pairing energy of the states with $|\mu| < g$ is lowered when the order parameter gets suppressed at $r < \xi$. It is clear from the figure, however, that the spectrum retains its general shape

even when the vortex has no normal core. In particular, the number of branches crossing the Fermi energy is always 1, in agreement with Volovik's theorem.

We have seen that suppressing the normal core, keeping only the supercurrent, does not change the core states qualitatively. We may now do the converse: in order to suppress the supercurrent and keep only the core, we set the phase of the order parameter to zero [i.e., $\nu = 0$ in Eqs. (3)–(5)] and we use the profile Eq. (6) with $\nu = 1$ and $r_c = \xi$. The resulting order parameter no longer describes a vortex, since the winding number vanishes, but just a normal region embedded in a uniform superconductor. The resulting spectrum (triangles in Fig. 1) is qualitatively different from the spectrum of a singly quantized vortex. Consistent with Volovik's result, no branch of core states cross the Fermi level, and therefore no low-energy states exist, although multiple Andreev reflections are, in principle, possible in this system. The suppression of the order parameter slightly decreases the pairing energy of the low-$|\mu|$ electron and hole excitations of the uniform superconductor and gives rise to two shallow branches of states near the gap edges.

Figure 2 compares the local density of states (LDOS) of a singly quantized vortex with and without normal core. As can be inferred from Fig. 1, the effect of the normal core is mainly to raise the peak at the vortex center, without changing the structure of the LDOS. The energy of the peak is also closer to the Fermi energy when the normal core is present. This is due to the core-induced energy change at low μ. Indeed, since only states with $\mu \pm \nu/2 = 0$ contribute to the LDOS at $r = 0$ [see Eq. (A1)], we have

$$N(0,E) \propto \sum_i \delta[E - E^i_{\mu = -(\nu/2)}] \quad (\nu \leqslant 0), \qquad (7)$$

where the index i corresponds to the various eigenvalues at fixed μ. Figure 2 also shows the LDOS of a normal core without supercurrent. In this case there is no zero-bias peak, but two sharp peaks near $\pm\Delta_\infty$ corresponding to the two branches in Fig. 1. These peaks disappear beyond a distance of order ξ and the LDOS becomes that of the uniform superconductor for $r > \xi$. In contrast, for a true vortex the perturbation to the bulk DOS extends to distances much larger than
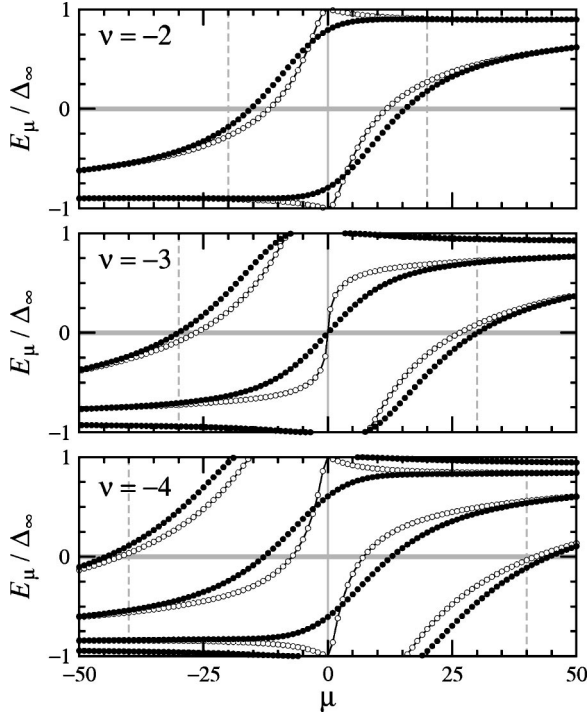
FIG. 3. Energy spectra for multiply quantized s-wave vortices. The black circles correspond to vortices having a normal core given by Eq. (6), and the white circles correspond to vortices without normal core. The dashed vertical lines delimit the region $|\mu| < |\nu| g$ where the levels are sensitive to the profile of the order parameter.

ξ, irrespective of the core radius r_c, due to the high-$|\mu|$ states in Fig. 1.

The vortex-core spectra and the LDOS of multiply quantized s-wave vortices ($|\nu| > 1$ were calculated in Ref. 12, using the self-consistent order-parameter profile. The number of branches crossing E_F was $|\nu|$ as expected. We have repeated these calculations using the profile Eq. (6) with both $r_c = \xi$ and $r_c = 0$. The results displayed in Fig. 3 show again that the order-parameter profile does not qualitatively change the core states. The overall shape of the spectra is determined by the strength of the supercurrent, which is proportional to the winding number. For odd ν, there is a branch crossing the Fermi energy at $\mu = 0$, while for even ν there is no such branch. In addition, other branches cross zero energy at higher angular momenta. The profile of $\Delta(r)$ affects the core states with $|\mu| < |\nu| g$. Except for small quantitative differences, the LDOS computed with and without the normal core are therefore very similar, as for the singly quantized vortex.

From Figs. 1 and 2 one sees that the presence of the supercurrent is a necessary and sufficient condition to have low-energy states (while the normal core is not), and from Fig. 3 one sees that the topological frustration, which is only present for odd ν, is a necessary condition to have low-energy *and* low-$|\mu|$ states, i.e., a zero-bias peak in the LDOS at the core center. In order to build a consistent explanation of the origin of the vortex-core states, it is thus necessary to understand the effect of the circulating superfluid on the BdG excitations.

B. Supercurrent and pairing energy

As already mentioned, the velocity field due to the supercurrent changes the angular momenta of the electron and hole parts of the BdG excitations in opposite ways. As a result, a phase difference of $\nu(\pi/2)$ is induced between the *radial* wave functions of the electron and hole. This phase difference is at the origin of the strong dependence of the vortex-core spectra on ν. One possible way to solve the BdG equations is to treat the modulus of the order parameter perturbatively, while taking full account of the phase. For a vanishing modulus, Eqs. (5a) decouple and the radial wave functions assume the simple form

$$\psi_\pm^0(\rho) = A_\pm J_{\mu \pm \nu/2}(g\sqrt{1 \pm \varepsilon}\rho),$$

where J is the Bessel function. The eigenvalues ε must be determined from the boundary condition at the border of a normalization disk of radius R, and they form a continuum for each value of μ as $R \to \infty$. The $\nu(\pi/2)$ phase shift can be easily seen from the asymptotic behavior of $J_m(x)$,

$$J_m(x) \sim \sqrt{\frac{2}{\pi x}} \cos\left[x - \left(m + \frac{1}{2}\right)\frac{\pi}{2}\right] \quad (x \gg m),$$

remembering that $\mu = n + (\nu/2)$ with integer n. The first-order perturbation theory in δ gives the energies of the core states as

$$\varepsilon_\mu = \varepsilon + 2\int_0^R d\rho\rho\,\delta(\rho)\psi_+^0(\rho)\psi_-^0(\rho).$$

Because of the phase shift, the pairing matrix element is qualitatively different for even and odd values of ν. For even ν and small ε, ψ_+^0 and ψ_-^0 are either in phase or out of phase by π, and the integrand is thus either positive or negative, leading to a maximal pairing energy of order Δ_∞. For odd ν, on the contrary, the integrand oscillates about zero and the resulting pairing energy is minimal. This mechanism is illustrated in Fig. 4, using the exact eigenstates rather than $\psi_\pm^0$. The solutions $\psi_\pm$ as well as the integrand of the pairing matrix element are displayed for the lowest allowed value of μ and for winding numbers $\nu = -1$ and -2. The numerical values of the kinetic and pairing energies, defined as

$$\varepsilon_{\text{kin}} = \langle\psi_+|L_+|\psi_+\rangle - \langle\psi_-|L_-|\psi_-\rangle$$

$$\varepsilon_{\text{pair}} = 2\langle\psi_+|\delta|\psi_-\rangle,$$

are also indicated.

The analysis of the numerical results at all angular momenta shows that the energy eigenvalues in Figs. 1 and 3 are dominated by the pairing energy. Due to the cancellation of the electron and hole contributions, the kinetic term remains small and has a weak μ dependence. The structure of the eigenvalue spectra and, in particular, the occurrence of low-energy states at high angular momentum for $|\nu| > 1$, can thus be qualitatively understood by considering the evolution of the pairing matrix element with μ. With increasing μ, an additional phase shift appears between the radial electron and hole wave functions at short distances [as can be seen from the functions $\psi_\pm^0(\rho)$, the phase shift always tends to $\nu\pi/2$
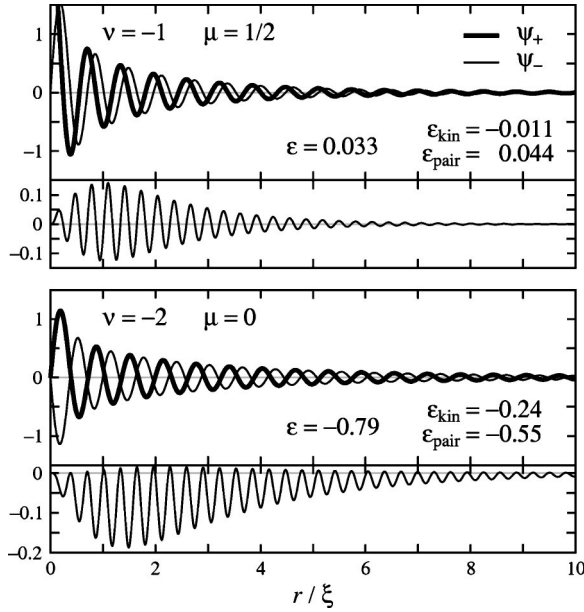
FIG. 4. Electron (ψ_+) and hole (ψ_-) BdG amplitudes for the lowest angular momentum in the singly (top) and doubly (bottom) quantized vortex with $r_c = \xi$. The integrand of the pairing matrix element, $\rho \tanh(\rho/\sqrt{|\nu|})^{|\nu|}\psi_+(\rho)\psi_-(\rho)$, is displayed in the bottom panels.

asymptotically, but it is a function of μ for $\rho < \mu/g$]. This has the effect of increasing the matrix element toward its maximum value of Δ_∞. For the lower branch in the $\nu = -2$ spectrum in Fig. 3, there is a $\mu > 0$ such that the total phase shift is close to $-(\pi/2)$, and the matrix element thus nearly vanishes.

In the Appendix, we derive an approximate solution for the bound states of the s-wave vortex. To lowest order in $\mu\nu/g\rho_c$ the eigenvalues are found to be

$$\frac{E_\mu}{\Delta_\infty} \approx \frac{-(\mu\nu/g\rho_c) + (2m + 1 + \nu)(\pi/2)}{1 + g\delta\rho_c}, \qquad (8)$$

where m is any integer such that $|E_\mu| < \Delta_\infty$ and ρ_c is some effective core radius in units of ξ. For $\nu = -1$, $g\delta = 2/\pi$, and $\rho_c = 1$, one recovers the famous Caroli–de Gennes–Matricon finding,[6] namely, that for each μ there is a unique solution within the gap ($m = 0$) with energy $E_\mu \approx \mu(\Delta_\infty^2/E_F)$.

The term $\nu(\pi/2)$ in Eq. (8) can be traced back to the phase difference discussed above (see the Appendix). Only for odd values of ν does the term in parentheses disappear for some m, hence a branch of bound states crosses the Fermi level at $\mu = 0$, contributing to the low-energy LDOS in the core. In this case the gap between the lowest-energy excitations in the core is $\Delta E_{\mu = \pm 1/2} = (\Delta_\infty^2/E_F)[\pi^2\nu/2\rho_c(\pi + 2\rho_c)]$, where ρ_c itself is a function of ν. The ν-dependence of $\Delta E_{\mu = \pm 1/2}$ may be estimated by demanding that the "hole" in $\Delta(\mathbf{r})$ in Eq. (6) and in the model calculation of the Appendix have identical volumes, namely $\pi\rho_c^2$. We then obtain $\rho_c^2 = 2|\nu|\int_0^\infty dx x(1 - \tanh^{|\nu|} x) \approx |\nu|^{2\alpha}$ with $\alpha = 0.78$. Hence $\Delta E_{\mu = \pm 1/2}$ is a decreasing function of $|\nu|$

$$\Delta E_{\mu = \pm 1/2} \approx \frac{\Delta_\infty^2}{E_F} \frac{|\nu|^{1-\alpha}}{2} \frac{\pi^2}{\pi + 2|\nu|^\alpha} \qquad (\nu \text{ odd}). \qquad (9)$$

For even values of ν there is always a large gap at $\mu = 0$, which is given by $\Delta E_{\mu = 0} = \Delta_\infty \pi/(1 + g\delta\rho_c)$ in this model. It should be noted that the presence (absence) of this large gap for even (odd) ν is due to the absence (presence) of the flux-induced topological frustration and does not depend on the order-parameter profile; however, the width of this gap does depend on the order-parameter profile through the effective core radius ρ_c. Using $\rho_c \approx |\nu|^\alpha$ and assuming the BCS relation $g\delta = 2/\pi$ holds, we find that $\Delta E_{\mu = 0}$ is also a decreasing function of $|\nu|$,

$$\Delta E_{\mu = 0} \approx \Delta_\infty \frac{\pi^2}{\pi + 2|\nu|^\alpha} \qquad (\nu \text{ even}), \qquad (10)$$

in good agreement with the numerical results in Fig. 3.

IV. ISOLATED D-WAVE VORTEX

Within the BdG theory, there is an important qualitative difference between the core spectra of isolated vortices in d-wave and s-wave superconductors. The energy spectrum of s-wave vortices is discrete (but looks continuous in experiments because of small inter-level spacing and thermal broadening), while numerical calculations suggest that the energy spectrum is continuous in the d-wave case,[19] although there are conflicting opinions in this respect.[20] The numerical solutions of the d-wave vortex lattice problem also point to a continuous spectrum of extended quasiparticle states.[21,22] A complete analytical solution would be useful to address this issue. The main difficulty comes from the nonlocality of the d-wave gap operator: gauge-invariant generalizations of the lattice d-wave gap to the continuum model are rather complicated.[23] In this section, the dependence of the core energy spectrum on the gap profile and vortex winding number is investigated numerically in the d-wave case. The issue of bound versus extended core states is not directly relevant here.

Instead of a continuum model we consider a two-dimensional nearest-neighbor lattice model. The vortex order parameter is taken to be

$$\Psi(\mathbf{r}_i, \mathbf{r}_j) = \begin{cases} \frac{1}{4}\Delta(|\mathbf{R}_{ij}|)\cos(2\tau_{ij})e^{i\nu\theta_{ij}} & \text{if } |\mathbf{r}_i - \mathbf{r}_j| = a \\ 0 & \text{otherwise,} \end{cases}$$

where $\mathbf{r}_i$ denotes a lattice site, a is the lattice parameter, $\mathbf{R}_{ij} = \frac{1}{2}(\mathbf{r}_i + \mathbf{r}_j) = |\mathbf{R}_{ij}|(\cos\theta_{ij}, \sin\theta_{ij})$, $\mathbf{r}_i - \mathbf{r}_j = a(\cos\tau_{ij}, \sin\tau_{ij})$, and $\Delta(r)$ is given by Eq. (6). This model order parameter is consistent with the self-consistent result.[19] As in the s-wave case, the small readjustments brought about by the self-consistency have practically no effect on the vortex spectrum. The LDOS in the core is calculated using the Green's function formalism

$$N(\mathbf{r}_i, E) = -\frac{2}{\pi}\text{Im } G_{ii}(E + i\Gamma). \qquad (11)$$
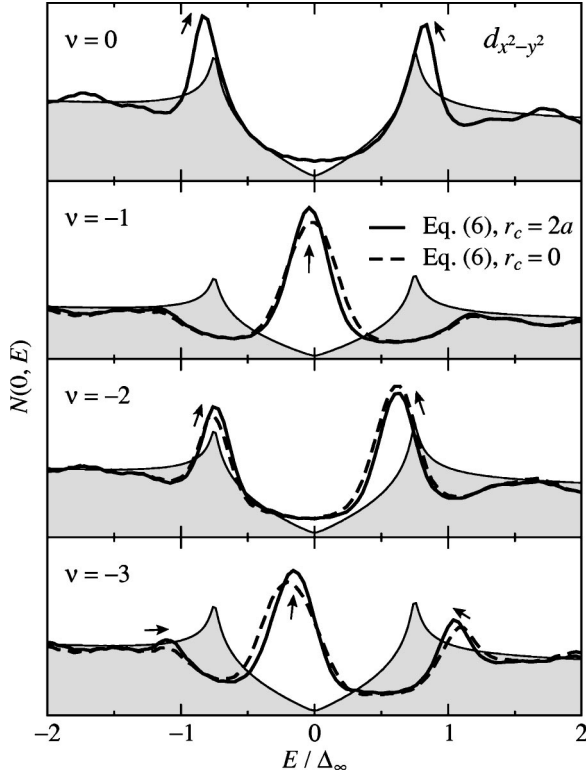
The Green's function is given by the Gorkov equations

FIG. 5. Local density of states in the core of d-wave vortices with increasing winding numbers. The solid lines correspond to vortices having a normal core given by Eq. (6), and the dashed lines correspond to vortices without normal core. The case $\nu=0$ corresponds to a normal core without supercurrent. The arrows show the displacement of the peak maxima when the system size increases from $M=41$ to $M=51$. The bulk DOS is shown in gray and provides a common scale to compare the spectra at different ν. Note that the bulk coherence peaks are not located at $E=\pm\Delta_\infty$ due to the large value of the chemical potential $\mu=t$.

$$G_{ij}(\omega) = G_{ij}^0(\omega) + \sum_{kl} G_{ik}^0(\omega)\Sigma_{kl}(\omega)G_{lj}(\omega) \quad (12a)$$

$$G_{ij}^0(\omega) = \frac{1}{N^2}\sum_{k} \frac{e^{i\boldsymbol{k}\cdot(\boldsymbol{r}_i-\boldsymbol{r}_j)}}{\omega - \varepsilon_{\boldsymbol{k}}} \quad (12b)$$

$$\Sigma_{ij}(\omega) = \sum_{kl} \Psi(\boldsymbol{r}_i,\boldsymbol{r}_k)G_{lk}^0(-\omega)\Psi^*(\boldsymbol{r}_l,\boldsymbol{r}_j) \quad (12c)$$

with N^2 the number of $\boldsymbol{k}$ points and $\varepsilon_{\boldsymbol{k}}$ the dispersion. The details of $\varepsilon_{\boldsymbol{k}}$ are not important in the context of this study. However, the presence of a van Hove singularity in the gap region provides additional spectral weight, which might be unequally distributed among the various peaks in the spectra, thus complicating their interpretation. In order to avoid such difficulties, the simple nearest-neighbor form $\varepsilon_{\boldsymbol{k}}=-2t(\cos k_x a+\cos k_y a)-\mu$ is used, with the chemical potential set to $\mu=t$ so that the van Hove singularity does not influence the spectra in the gap region. Eq. (12) is solved by first computing $G_{ij}^0(\omega)$ for a large system ($N=1024$), taking advantage of the translational invariance in Eq. (12b). Then the inhomogeneous terms $\Sigma_{ij}(\omega)$ and $G_{ij}(\omega)$ are calculated on a
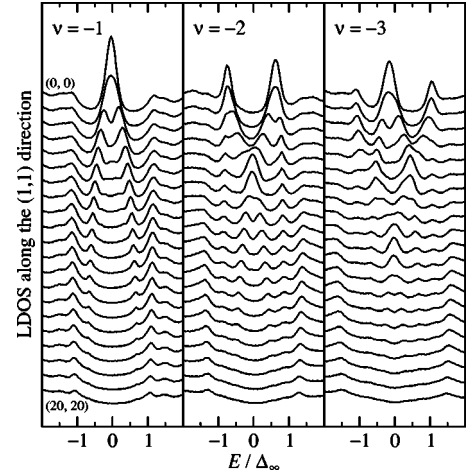

FIG. 6. LDOS along the nodal direction for d-wave vortices of increasing winding numbers. The curves show the LDOS at all sites between (0, 0) and (20, 20), and are offset vertically for clarity.

smaller $M \times M$ system ($M=51$) with the vortex at the center. With this method the finite-size effects do not contaminate the free propagator, and a good spectral resolution can be achieved. The hopping integral is set to $t=5\Delta_\infty$ (a value typical for high-T_c materials) and the energy broadening is $\Gamma=\Delta_\infty/50$.

The LDOS calculated at the vortex center with $r_c=2a$ and $r_c=0$ and for various winding numbers is displayed in Fig. 5. The LDOS for a "normal core" of radius $2a$ without supercurrent is also shown and denoted as $\nu=0$. One can see several striking similarities with the s-wave vortex. For $|\nu|\geq1$, the suppression of the order parameter has a very small effect on the LDOS in the core. This is confirmed by the case $\nu=0$, which shows that a local suppression of $\Delta(r)$ is unable to induce low-energy states. (The small flat DOS at $E=0$ for $\nu=0$ and $\nu=-2$ is probably a finite-size effect.[24]) For $\nu=0$, there is a transfer of spectral weight from high to low energy at $E\approx\Delta_\infty$, resulting in two sharp states near the gap edges. Increasing the system size from $M=41$ to $M=51$, these states sharpen while moving to slightly lower binding energy, as indicated by the small arrows in the figure. At convergence, these states would presumably lie within the bulk gap, as in the s-wave case. For $|\nu|\geq1$, one observes a strong even-odd effect. Vortices with odd ν have a zero-bias conductance peak (ZBCP), which is absent in even vortices. The ZBCP sharpens with increasing system size, but its energy is well converged at the system size considered. For $|\nu|\geq2$, there are additional states at high energy, which are the analogs of the high-energy states near $\mu=0$ in the s-wave case (see Fig. 3). One can observe that the sensitivity of the peaks to system size increases with energy, suggesting that the states at higher energy are less localized.

In the neighborhood of the vortex axis, the LDOS has many characteristics in common with the LDOS of s-wave vortices. In Fig. 6, one can see that in the case $\nu=-1$ the ZBCP at the core center splits into two symmetric peaks at larger distances, very much like the high angular momentum electron-hole excitations in the s-wave case (compare Fig. 2). These excitations have been the focus of a recent self-

consistent calculation.[25] In the doubly quantized vortex, the two peaks near the gap edges vanish slowly as the distance from the core increases, while a ZBCP develops, which is maximum at a distance $r=5\sqrt{2}a$. The latter again decomposes into two symmetric excitations at larger distances. The resulting LDOS is thus very similar to that of a doubly quantized s-wave vortex (see Fig. 4 of Ref. 12), and can be readily interpreted on the basis of Fig. 3. A similar analysis shows that all of the features of the s-wave vortex with $\nu=-3$ (Fig. 4 of Ref. 12) can be distinguished in the LDOS of the $\nu=-3$ d-wave vortex (Fig. 6). The LDOS exhibits some anisotropy around the vortex, but the differences between the nodal and antinodal directions are small. In particular, all the features discussed in Fig. 6 are also present in the antinodal direction.

V. PERTURBATIONS OF THE ORDER-PARAMETER PHASE

The results of the previous sections suggest that the core states have a topological origin. An implication of this is that the states must not be suppressed by changes in the phase of the order parameter, as long as these changes preserve the topological defect. Conversely, the core states should be strongly affected by the interaction with an antivortex, since the latter annihilates the effect of the topological defect on orbits larger than the vortex-antivortex distance. In this section, we investigate the effects of some perturbations of the phase field on the core states in a d-wave superconductor, starting with the perturbation induced by a nearby antivortex.

The order parameter for a vortex-antivortex pair was taken as the normalized product of the order parameters associated with each constituent (i.e., two vortices with winding numbers 1 and -1 and $r_c=2a$). The vortex is located at the origin and the antivortex at position $\boldsymbol{b}=(-b,-b)$. In Fig. 7 is shown the LDOS at the vortex center and along the diagonal, in the direction opposite to the vortex-antivortex direction. The phase field around the vortex is also displayed. For $b=20a$, the LDOS is similar to the LDOS of an isolated singly quantized vortex (Fig. 6). However, although the phase field is barely modified by the antivortex in the region where the LDOS is calculated, the latter is considerably broadened: the height of the ZBCP is only 71% of the corresponding height in the isolated vortex, while the gap integrated spectral weight is conserved within 2%. Note also that the ZBCP is already split at site (1, 1), unlike in the isolated case where this splitting occurs first at site (2, 2). Reducing the vortex-antivortex distance ($b=10a$), the ZBCP at site (0, 0) also splits. At the same time, the energy separation between the two states away from the core center is increased. Finally, at $b=2a$ the ZBCP disappears completely and the LDOS resembles the LDOS of a $\nu=0$ "vortex" (see Figs. 5 and 2).

The spectra in Fig. 7 show that the formation of the core states is a nonlocal process: the LDOS at a particular site depends on the phase winding in a region much larger than the core radius r_c. In fact the height of the ZBCP at (0, 0) reaches 95% of its value in the isolated vortex for vortex-antivortex separations as large as $\sim 70a$ ($b=50a$). This value
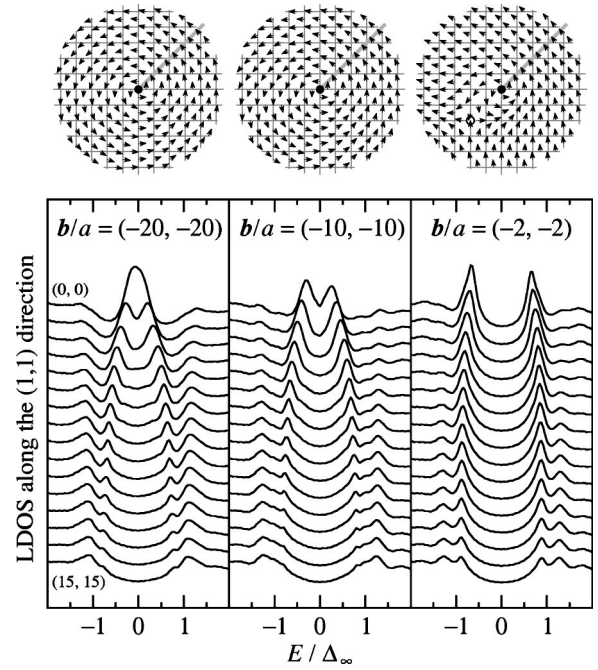

FIG. 7. LDOS along the nodal direction (indicated by a thick gray line in the top part) for a vortex-antivortex pair in a d-wave superconductor for various vortex-antivortex separations. The antivortex (white dot, only visible at the shortest distance) is at position $\boldsymbol{b}$ with respect to the vortex (black dot). The order-parameter phase in the region of the vortex center (excluding the $d_{x^2-y^2}$ symmetry factor for clarity) is represented in the form of a small arrow on each bond of the square lattice.

sets an upper bound for the size of the aforementioned region. On the other hand, a clear splitting of the ZBCP at site (0, 0) occurs for $b=19a$ or less, which sets a lower bound to $27a$. These numbers can be compared with the spatial extension of the core states. In the s-wave vortex the latter is typically $\ell \approx 2E_F/(k_F\Delta_\infty)$ for a state at $E=0$ [see Eq. (A3)]. Using $E_F=5t$ (the position of the Fermi energy with respect to the bottom of the band in the calculations), $k_F=\pi/(2a)$, and $t=5\Delta_\infty$ one obtains $\ell \approx 32a$, which falls within the bounds deduced from the numerical simulations. Thus, although the typical localization radius of the bound states might be different in d-wave and s-wave superconductors,[19] one may conclude that the LDOS in the vortex core "feels" the presence of an antivortex (or another vortex in a vortex lattice) at any distance shorter than the extension of the bound states.

The sensitivity of the LDOS to perturbations of the phase that preserve the topological defect was studied by randomly disordering the phase field, i.e., replacing the order parameter Ψ of the isolated vortex by Ψe^{ix} where x is a random Gaussian variable centered at $x=0$ with variance W (full width at half maximum). The resulting LDOS is displayed in Fig. 8. At $W=\pi/8$ and $W=\pi/4$, the spectra are practically unchanged with respect to the ordered case. No new structure is induced in the spectra up to the strongest disorder considered. At $W=\pi/2$, though, the ZBCP is reduced (but *not* broadened) and the energy separation between the two electron-hole excitations away from the core is decreased.
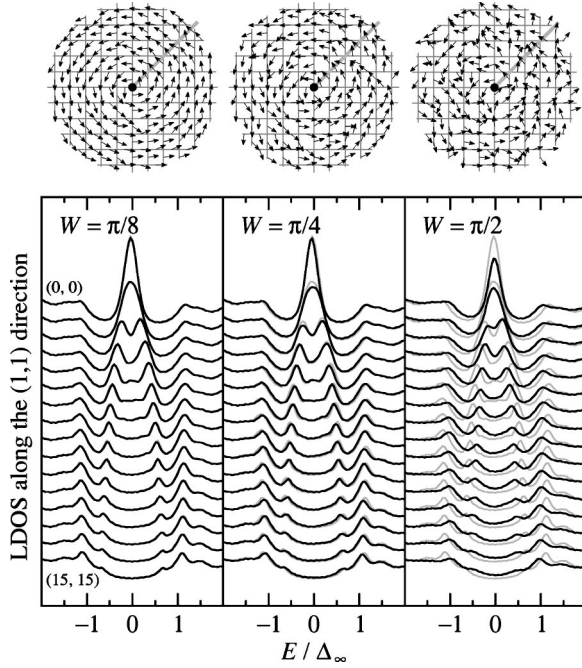
FIG. 8. LDOS along the nodal direction for a d-wave singly-quantized vortex subject to random phase disorder. W characterizes the strength of disorder. The phase field in the core region is shown in the top part. The spectra corresponding to the ordered case (W =0) are shown in grey for comparison.

This might be attributed to the loss of rotational symmetry, which leads to a stronger interaction between angular momentum eigenstates, and to a redistribution of spectral weight. We note that the integrated LDOS is conserved within 3% at all sites and for all disorder strengths considered.

VI. DISCUSSION

The numerical results reported in Figs. 2 and 5 imply that the suppression of the modulus $\Delta(r)$ of the order parameter in the core can be safely ignored when discussing the mechanism of formation of the vortex states in s- and d-wave superconductors. The main reason is the small magnitude of the superconducting gap with respect to the Fermi energy: a local suppression of $\Delta(r)$ is a *very weak* perturbation for excitations at the Fermi surface, which does not provide a substantial gain of pairing energy for a localized Bogoliubov excitation (unless the localization radius is smaller than the core radius, which, in turn, costs a large kinetic energy). Making use of Eq. (8) with $\nu=0$, one can see that a local suppression of $\Delta(r)$ can induce low-energy states in the limit $\Delta_\infty/E_F \gg (k_F r_c)^{-1}$, which is never attained in the BCS superconductors for which $\Delta_\infty/E_F \approx 2/\pi(k_F r_c)^{-1}$.

Thus the origin of the bound states must be searched in the phase $\chi(r)$ of the order parameter. Far from the vortex, the slow variation of $\chi(r)$ is known to induce a small density of states in the gap by the Doppler-shift effect.[26] The Doppler-shift approximation is not valid in the core region because there the superfluid velocity is too large, but also

because this approximation neglects the topological defect associated with the phase winding. A comparison of the right panels in Figs. 7 and 8 unambiguously shows that the microscopic details of $\chi(r)$ are much less relevant to the formation of the vortex LDOS than the "macroscopic" phase winding. This is further evidenced by the qualitative differences between even-ν and odd-ν vortices. The mechanism described in Sec. III B provides a natural explanation to these results, since the interference between the electron and the hole, which is responsible for the formation of the bound states, is a global property of the wave function and is not destroyed by local perturbations of $\chi(r)$. The issue of self-consistency in the order parameter (modulus and phase) is one of the major obstacles to a complete analytical calculation of the vortex-core LDOS. Nevertheless, the results of the present study suggest that the LDOS calculated from the simplest possible "trial" order parameter, i.e., a uniform modulus $\Delta(r,\theta) \equiv \Delta_\infty$ and a geometric phase $\chi(r,\theta) = \nu\theta$, should exhibit all the characteristic features of the exact solution. (An interesting exception might be the case where subdominant order parameters of different symmetries are brought about by the self-consistency.)

In the presence of several topological defects, the winding ν in Eq. (1) depends on the number of defects contained in the path of integration. Based on the analysis in Sec. V, we tentatively argue that the structure of the vortex core LDOS is determined primarily by the average vorticity in the region occupied by the core states. This statement was checked by considering a variety of vortex and antivortex configurations. For example, the effect of a $\nu=2$ antivortex on the LDOS in the core of a $\nu=-1$ vortex was studied. The antivortex was located at position $\boldsymbol{b}=(-b,-b)$ as in Fig. 7. For small (b/a <2) and large ($b/a \gtrsim 20$) vortex-antivortex separations the LDOS was found to be close to that of an isolated vortex. Near $b=5a$ the spectrum was similar to the topmost case in Fig. 5, corresponding to $\nu=0$. Finally, in the other regions the LDOS exhibited intermediate shapes. In this geometry the vorticity is -1 in the region $r < b\sqrt{2}$ and $+1$ in the region $r > b\sqrt{2}$, so that the average vorticity in a region of radius R is $\bar{\nu} = 1-4(b/R)^2$ if $b\sqrt{2} < R$ and -1 if $b\sqrt{2} > R$. Thus $|\bar{\nu}| \approx 1$ for small and large b, whereas $|\bar{\nu}| \approx 0$ for $b \sim R/2$.

In the normal state of the superconducting cuprates, the behavior of the high-frequency optical conductivity[27] and the presence of a large Nernst signal[28] have been generally attributed to vortex excitations, in the form of unbound vortex-antivortex pairs. Recently, Lee[29] argued that such vortices have to be "cheap," i.e., must be free of core states in order to have a formation energy comparable to the thermal energy $\sim k_B T_c$. Experimentally, there is indeed convincing evidence from scanning tunneling microscope (STM)[30–33] and NMR[34,35] measurements that the core states are suppressed at $T < T_c$ in the cuprates, pointing to a failure of the simple d-wave BCS theory in the superconducting state. Lee pointed out that a straightforward extension of the BCS theory that includes phase fluctuations is unable to produce "cheap" vortices in the normal state. This argument relies on the assumption that the average vortex-core LDOS in a vortex-antivortex soup is similar to the LDOS of an isolated vortex. As Fig. 7 shows, however, the vortex-core states can be very

efficiently suppressed in a "BCS" vortex-antivortex pair, even when the vortex-antivortex separation is much larger than the core radius. It is likely that the same phenomenon also occurs in more sophisticated models of the high-T_c superconductors. A systematic investigation of the core energy as a function of the vortex density in a state of fluctuating vortex-antivortex pairs would thus be helpful to elucidate the nature of the normal state in the cuprates.

In this study, the effect of the order-parameter symmetry on the properties of the vortex states was left aside and the emphasis was put on the similarities of the LDOS in s- and d-wave vortices, which illustrates the key role of the vorticity in both cases. It is well known that a subdominant order parameter can induce qualitative changes in the LDOS of BCS vortices.[19] Furthermore, the delicate question of the spatial extension of the core states in the d-wave case (exponentially localized or extended) was not addressed. These issues are a good motivation to search for a realistic analytical solution of the BdG equations for vortices in superconductors with nonlocal pairing.

VII. CONCLUSION

In the BCS theory, the superconducting state is characterized by a complex order parameter, with a modulus $\Delta(\mathbf{r})$ related to the superfluid density and a phase $\chi(\mathbf{r})$ related to the supercurrent. Although the electronic states bound to vortices have often been attributed to the suppression of the superfluid density in the core region, it was found that the bound states are completely formed when this suppression is overlooked, which confirms an earlier finding based on the quasiclassical approximation.[11] In order to explain the formation of the core states, a mechanism was proposed that relies on the influence that the vortex supercurrent exerts on the Bogoliubov excitations. In short, the Bogoliubov excitations localize onto vortices because the *topology* of the latter—not the normal core—gives to the electron and hole components the possibility to avoid one another and to minimize their pairing energy. The spectral properties of vortices carrying more than one flux quantum, as well as of vortex-antivortex pairs, are consistent with this idea. The proposed mechanism of localization results from the particular form of the coupling mediated by the supercurrent between the electron and hole components and is therefore unique to superconductors.

APPENDIX: APPROXIMATE SOLUTION FOR THE *S*-WAVE VORTEX

In this appendix an approximate solution of the BdG equations for an isolated vortex in a s-wave superconductor is derived. This solution differs somewhat from those given in Refs. 6 and 7 and applies to vortices of arbitrary winding number ν. The purpose here is to highlight the role of ν on the vortex-core spectrum. The radial wave function is written as

$$\psi_{\pm}(\rho) = \mathrm{Re}\, H_{\mu \pm \nu/2}(g_{\pm}\rho) f_{\pm}(\rho), \qquad (A1)$$

where $g_{\pm} = g\sqrt{1 \pm \varepsilon}$ and $H_n(x) = J_n(x) + iY_n(x)$ with J and Y the Bessel functions of the first and second kind, respectively. Equation (5) becomes

$$\pm \frac{1}{g^2} \left[-\frac{d^2}{d\rho^2} - \left(\frac{1}{\rho} + 2\frac{H'_{\pm}}{H_{\pm}} \right) \frac{d}{d\rho} \right] f_{\pm} + \delta(\rho) \frac{H_{\mp}}{H_{\pm}} f_{\mp} = 0.$$
$$(A2)$$

$H_{\mu \pm \nu/2}(g_{\pm}\rho)$ is abbreviated as $H_{\pm}$, and $H'_{\pm} = dH_{\pm}/d\rho$. At this point we make two simplifications: (i) We consider a square gap profile: $\delta(\rho) = \delta\theta(\rho - \rho_c)$. As shown in the main text, the vortex-core spectrum is only weakly influenced by the details of $\delta(\rho)$. (ii) We use the approximations

$$\frac{1}{\rho} + 2\frac{H'_{\pm}}{H_{\pm}} \approx 2ig_{\pm}$$

$$\frac{H_{\mp}}{H_{\pm}} \approx \sqrt{\frac{g_{\pm}}{g_{\mp}}} e^{\pm i\nu\pi/2} \left(1 \mp i\frac{\mu\nu}{\rho_c} \frac{g_+ + g_-}{2g_+g_-} \right) e^{\mp i(g_+ - g_-)\rho}.$$

These expressions were obtained from the asymptotic form of the Bessel functions

$$H_n(x) \approx \sqrt{\frac{2}{\pi x}} e^{i[x + (n^2/2x) - (n+1/2)\pi/2]} \quad (x > n),$$

by expanding to first order in μ/g and ν/g. Approximation (ii) is therefore inadequate for $\mu \pm \nu/2 > g$. Furthermore, in the second line, the term proportional to $1/\rho$ was evaluated at $\rho = \rho_c$. This is justified for the calculation of the eigenvalues, since the latter are determined by matching the wave functions at $\rho = \rho_c$. Note also that this approximation will break down if $\rho_c \ll 1$. The factor $e^{\pm i\nu(\pi/2)}$ in the expression for $H_{\mp}/H_{\pm}$ is the consequence of the phase shift discussed in Sec. III B. With these simplifications Eq. (A2) can be solved exactly. We restrict the analysis to subgap states with $\varepsilon < \delta$. At $\rho < \rho_c$ the solution is simply $f_{\pm}^{<}(\rho) = A_{\pm}$ where $A_{\pm}$ are real constants. At $\rho > \rho_c$, the solution can be written as

$$f_{\pm}^{>}(\rho) = B_{\pm} e^{i(q - g_{\pm})(\rho - \rho_c)} e^{-k(\rho - \rho_c)} \qquad (A3)$$

with $q = g(\zeta + \frac{1}{2})^{1/2}$, $k = g(\zeta - \frac{1}{2})^{1/2}$, $\zeta = \frac{1}{2}(1 + \delta^2 + \gamma^2 - \varepsilon^2)^{1/2}$, and $\gamma = \delta[(g_+ + g_-)\mu\nu/2g_+g_-\rho_c]$. The $B_{\pm}$ are complex numbers and they are related by

$$\frac{B_-}{B_+} = \sqrt{\frac{g_-}{g_+}} \frac{\varepsilon - i\sqrt{4\zeta^2 - 1}}{\delta - i\gamma} e^{i[(g_+ - g_-)\rho_c - \nu(\pi/2)]}. \qquad (A4)$$

Introducing the solutions $f_{\pm}^{<}$ and $f_{\pm}^{>}$ into Eq. (A1) and matching the wave function and its derivative at $\rho = \rho_c$ one obtains

$$\frac{B_s}{A_s} = 1 - \frac{[kJ_s + (q - g_s)Y_s](Y_s + iJ_s)}{(q - g_s)(J_s^2 + Y_s^2) - (Y_sJ'_s - J_sY'_s)}, \qquad (A5)$$

with $s = \pm$, $J_{\pm} = J_{\mu \pm \nu/2}(g_{\pm}\rho_c)$, and $Y_{\pm} = Y_{\mu \pm \nu/2}(g_{\pm}\rho_c)$. Equations (A4) and (A5) provide the relation between the coefficients A_+ and A_-, as well as the eigenvalue equation

$$\tan\left[(g_+ - g_-)\rho_c - \nu\frac{\pi}{2}\right] = \frac{-\varepsilon + \eta\sqrt{\delta^2 + \gamma^2 - \varepsilon^2}}{\varepsilon\eta + \sqrt{\delta^2 + \gamma^2 - \varepsilon^2}}, \quad (A6)$$

where

$$\eta = \frac{\delta + \alpha\gamma}{\gamma - \alpha\delta}, \quad \alpha = \tan\arg\frac{B_-/A_-}{B_+/A_+}.$$

In Eq. (A6) $g_\pm$, γ, and η are all functions of ε. In order to make Eq. (A6) more tractable, we note that $\zeta \approx \frac{1}{2}$ and $g_\pm \approx g$ since δ, γ, and ε are small numbers. Taking $\zeta = \frac{1}{2}$ and $g_\pm = g$ in Eq. (A5) we obtain $B_s/A_s = 1$ and therefore $\alpha = 0$. Equation (A6) can then be solved to first order in ε

$$\frac{\varepsilon}{\delta} = \frac{E}{\Delta_\infty} \approx \frac{-\tan^{-1}(\mu\nu/g\rho_c) + (2m + 1 + \nu)(\pi/2)}{[1 + (\mu\nu/g\rho_c)^2]^{-1/2} + g\delta\rho_c}$$

$$\approx \frac{-(\mu\nu/g\rho_c) + (2m + 1 + \nu)(\pi/2)}{1 + g\delta\rho_c}, \quad (A7)$$

where m is any integer such that $|E| < \Delta_\infty$ and the second line is valid to first order in $\mu\nu/g\rho_c$. We have checked numerically that the eigenvalues resulting from Eqs. (A6) and (A7) are in excellent agreement at all μ. Equation (A7) correctly accounts for the qualitative difference between odd-ν and even-ν vortices. Due to the approximations made, however, the validity of Eqs. (A6) and (A7) is limited to the region $|\mu\nu| < g$, and the zero-energy states at $|\mu| \gtrsim g$ in Fig. 3 are not reproduced.

[1] G. Blatter, M. V. Feigel'man, V. B. Geshkenbein, A. I. Larkin, and V. M. Vinokur, Rev. Mod. Phys. **66**, 1125 (1994).

[2] R. P. Huebener, N. Schopohl, and G. E. Volovik, eds., *Vortices in Unconventional Superconductors and Superfluids* (Springer, Berlin, 2002).

[3] See e.g.: A. S. Melnikov, Phys. Rev. Lett. **86**, 4108 (2001).

[4] See e.g.: L. F. Chibotaru, A. Ceulemans, V. Bruyndoncx, and V. V. Moshchalkov, Nature (London) **408**, 833 (2000).

[5] A. S. Mel'nikov and V. M. Vinokur, Nature (London) **415**, 60 (2002).

[6] C. Caroli, P. G. de Gennes, and J. Matricon, Phys. Lett. **9**, 307 (1964).

[7] J. Bardeen, R. Kümmel, A. E. Jacobs, and L. Tewordt, Phys. Rev. **187**, 556 (1969).

[8] H. F. Hess, R. B. Robinson, R. C. Dynes, J. M. Valles, and J. V. Waszczak, Phys. Rev. Lett. **62**, 214 (1989).

[9] F. Gygi and M. Schlüter, Phys. Rev. B **41**, 822 (1990); Phys. Rev. Lett. **65**, 1820 (1990); Phys. Rev. B **43**, 7609 (1991).

[10] D. Rainer, J. A. Sauls, and D. Waxman, Phys. Rev. B **54**, 10 094 (1996).

[11] G. E. Volovik, JETP Lett. **57**, 244 (1993).

[12] S. M. M. Virtanen and M. M. Salomaa, Phys. Rev. B **60**, 14 581 (1999).

[13] M. Stone, Phys. Rev. B **54**, 13 222 (1996).

[14] S. Hofmann and R. Kümmel, Phys. Rev. B **57**, 7904 (1998).

[15] G. Toulouse and M. Kléman, J. Phys. (Paris) **37**, 149 (1976).

[16] M. Franz and Z. Tešanović, Phys. Rev. Lett. **84**, 554 (2000).

[17] The wave functions were normalized on a disk of radius $R = 100\xi$.

[18] G. Lasher, Phys. Rev. **140**, A523 (1965); **154**, 345 (1967).

[19] M. Franz and Z. Tešanović, Phys. Rev. Lett. **80**, 4763 (1998).

[20] Y. Morita, M. Kohmoto, and K. Maki, Phys. Rev. Lett. **78**, 4841 (1997); Europhys. Lett. **40**, 207 (1997).

[21] Yong Wang and A. H. MacDonald, Phys. Rev. B **52**, R3876 (1995).

[22] Kouji Yasui and Takafumi Kita, Phys. Rev. Lett. **83**, 4168 (1999).

[23] O. Vafek, A. Melikyan, M. Franz, and Z. Tešanović, Phys. Rev. B **63**, 134509 (2001).

[24] The LDOS at $E=0$ in the case $\nu=0$ ($\nu=-2$) decreases by 27% (28%) when increasing system size from $M=51$ to $M=71$.

[25] J.-X. Zhu, C. S. Ting, and A. V. Balatsky, cond-mat/0109503 (unpublished).

[26] G. E. Volovik, JETP Lett. **58**, 469 (1993).

[27] J. Corson, R. Mallozzi, J. Orenstein, J. N. Eckstein, and I. Bozovic, Nature (London) **398**, 221 (1999).

[28] Z. A. Xu, N. P. Ong, Y. Wang, T. Kakeshita, and S. Uchida, Nature (London) **406**, 486 (2000).

[29] P. A. Lee, Physica C **388**, 7 (2003).

[30] I. Maggio-Aprile, Ch. Renner, A. Erb, E. Walker, and Ø. Fischer, Phys. Rev. Lett. **75**, 2754 (1995).

[31] Ch. Renner, B. Revaz, K. Kadowaki, I. Maggio-Aprile, and Ø. Fischer, Phys. Rev. Lett. **80**, 3606 (1998).

[32] S. H. Pan, E. W. Hudson, A. K. Gupta, K.-W. Ng, H. Eisaki, S. Uchida, and J. C. Davis, Phys. Rev. Lett. **85**, 1536 (2000).

[33] B. W. Hoogenboom, K. Kadowaki, B. Revaz, M. Li, Ch. Renner, and Ø. Fischer, Phys. Rev. Lett. **87**, 267001 (2001); B. W. Hoogenboom, Ch. Renner, B. Revaz, I. Maggio-Aprile, and Ø. Fischer, Physica C **332**, 440 (2000).

[34] V. F. Mitrović, E. E. Sigmund, M. Eschrig, H. N. Bachman, W. P. Halperin, A. P. Reyes, P. Kuhns, and W. G. Moulton, Nature (London) **413**, 501 (2001).

[35] K. Kakuyanagi, K. Kumagai, and Y. Matsuda, Phys. Rev. B **65**, 060503 (2002).